Supporting Information

Ibrahim et al. 10.1073/pnas.0912632107

SI Materials and Methods

Reverse Transcriptase–PCR (RT-PCR) Analyses. Total RNA was isolated with TRI reagent and contaminant DNA was removed by DNase-I treatment (Ambion). First-strand cDNA synthesis and PCR reactions were performed as previously described (1, 2). PCR products were resolved on 2% agarose gels and visualized by ethidium bromide staining (2). The number of cycles showing a linear relationship between input RNA and the final product was determined in preliminary experiments. Controls included the use as template of reactions without RT and verification of PCR products by hybridization with specific probes (data not shown). The primer sequences were as follows: for *AGO1*, AGO1-F (5′-CTTCGTGGTGGTCCAGAAGTC-3′) and AGO1-R (5′-CACCATGTACCGCAGTGTGC-3′); for *AGO2*, AGO2-F (5′-GTCCTAGCGGAGGAGTTCACG-3′) and AGO2-R (5′-TGATGCCACTGTCCACCACC-3′); for *AGO3*, AGO3-F (5′-GGGCACTGTGGTGGACAGC-3′) and AGO3-R (5′-CGCGGTCGGCGTAGTAGG-3′); for *RRP6a*, Rrp6a-sca27-F3 (5′-ACTTCCGGCTGTATCTGGTGAA-3′) and Rrp6a-sca27-R3 (5′-CCTTGTCTGCGGCCATGT-3′); for *RRP6b*, Rrp6b-sca11-F3 (5′-GGCTACGTGCTGCCCAAG-3′) and Rrp6b-sca11-R4 (5′-CGTCACCACCTCAGACACG-3′); and for *ACT1*, ACT-cod-F (5′-GACATCCGCAAGGACCTCTAC-3′) and ACT-cod-R (5′-GATCCACATTTGCTGGAAGGT-3′).

Small RNA Library Construction and Data Analysis. The small RNA fraction was precipitated from 800 μg of total RNA and cDNA libraries were constructed as previously described (3). The 5′ RNA adapters contained unique 2-nt additional barcodes at their 3′ termini (GA, UC, AG, and CU for the Mut-68–1, Mut-68–2, Maa7-IR44–1, and Maa7-IR44–2 libraries, respectively). Equal amounts of the final DNA products from each library were pooled and sequenced by Illumina. After sequencing, the adapter sequences were removed and remaining sequence reads binned according to their barcodes. Sequences shorter than 18 nt or longer than 28 nt were discarded. Sequence reads were compared to the *C. reinhardtii* genome versions 3.1 and 4.0, ESTs, predicted transcripts, transposons, and bonus reads (http://genome.jgi-psf.org/Chlre4/Chlre4.download.ftp.html) (4). Sequences matching tRNAs, rRNAs, snRNAs, snoRNAs (5), the chloroplast or the mitochondrial genomes were removed as these were likely to be degradation products. The remaining sRNAs were normalized to transcripts per million (TPM) and grouped into different categories. Phased siRNAs were characterized as sRNAs matching previously described phased loci (6, 7). To identify potential miRNAs, the *Chlamydomonas* miRNAs in the miRBase database (http://microrna.sanger.ac.uk/sequences) were matched to genome version 4.0. Because many *Chlamydomonas* miRNAs did not have reported miRNA* sequences in the Sanger database, the genomic regions were folded using mFOLD (8) and the miRNA* sequences retrieved. Sequence reads matching genome version 4.0 with 5′ ends +/− 1 nt relative to the 5′ end of a reported miRNA or miRNA* were considered miRNAs or miRNA*s, respectively. This was expanded to a 5-nt offset for the data reported in each miRNA cluster (Table S5 in Dataset S1). In cases where the miRNA or miRNA* resided in more than one locus in the genome, the small RNA profiles were compared for each locus and only unique profiles are displayed (Table S5 in Dataset S1). To identify sRNAs with 1- or 2-nt untemplated tails, the first 18 nt of the small RNAs were matched to the genome. Sequences with a perfect match were then extended until a mismatch was found. To minimize including reads with sequencing errors as having 3′ untemplated nucleotides, if the nucleotides after the first mismatch matched the genome, the sRNAs were not considered to be tailed. The deep sequencing libraries are deposited in NCBI GEO (GSE17815).

Analysis of the Chemical Nature of Small RNA Ends. Twenty micrograms of YM-100–enriched small RNAs were used for each reaction. Periodate oxidation and β-elimination of RNAs were carried out as described (9). Some reactions were spiked with an unmodified, 31-nt synthetic oligoRNA (2726 substrate, 5′-ACAUACACCUGGUCCCGCUACCUGAAAUACA-3′). To probe the sRNA 5′ ends, samples were treated with 2 units terminator exonuclease, an enzyme that digests RNAs with a free 5′ monophosphate, following the manufacturer's instructions (Epicentre). Small RNAs were also incubated with 10 units antarctic phosphatase (New England Biolabs) to remove terminal phosphate groups (10). Some small RNA samples, subjected to dephosphorylation, were also resuspended in RNase-free water and then treated with T4 polynucleotide kinase (New England Biolabs).

Transient Expression and Analysis of MUT68:GUS Subcellular Localization in Onion Epidermal Cells. Because recombinant proteins are poorly expressed in *Chlamydomonas* (11), onion epidermal peels were used as a transient expression system, consisting of transparent cells that facilitate subcellular imaging. A fusion protein between MUT68 and *E. coli* β-glucuronidase, under the control of the cauliflower mosaic virus 35S promoter, was constructed as previously described (12). Cells in the epidermal layer of onion bulbs were transformed by microprojectile bombardment with DNA coated tungsten particles (13). After bombardment the epidermal peels were incubated for 18–20 h at 23 °C under constant light of 50 $\mu mol \cdot m^{-2} \cdot s^{-1}$ photosynthetically active radiation. Cell layers were stained for GUS activity as described (13), washed briefly in 100 mM sodium phosphate (pH 7.0), and mounted in the same solution containing 1 $\mu g\ mL^{-1}$ propidium iodide (PI) (12). The stained cells were inspected by bright-field microscopy for distribution of GUS activity and by epifluorescent microscopy for PI labeling of the nucleus (12).

1. Rohr J, Sarkar N, Balenger S, Jeong B-R, Cerutti H (2004) Tandem inverted repeat system for selection of effective transgenic RNAi strains in *Chlamydomonas*. *Plant J* 40:611–621.
2. Sambrook J, Russell DW (2001) *Molecular Cloning – A Laboratory Manual* (Cold Spring Harbor Laboratory Press, Cold Spring Harbor, NY).
3. Lu C, Meyers BC, Green PJ (2007) Construction of small RNA cDNA libraries for deep sequencing. *Methods* 43:110–117.
4. Jain M, et al. (2007) EST assembly supported by a draft genome sequence: an analysis of the Chlamydomonas reinhardtii transcriptome. *Nucleic Acids Res* 35:2074–2083.
5. Chen C-L, et al. (2008) Genomewide analysis of box C/D and box H/ACA snoRNAs in Chlamydomonas reinhardtii reveals an extensive organization into intronic gene clusters. *Genetics* 179:21–30.
6. Molnár A, Schwach F, Studholme DJ, Thuenemann EC, Baulcombe DC (2007) miRNAs control gene expression in the single-cell alga *Chlamydomonas reinhardtii*. *Nature* 447:1126–1129.
7. Zhao T, et al. (2007) A complex system of small RNAs in the unicellular green alga *Chlamydomonas reinhardtii*. *Genes Dev* 21:1190–1203.
8. Zuker M (2003) Mfold web server for nucleic acid folding and hybridization prediction. *Nucleic Acids Res* 31:3406–3415.
9. Alefelder S, Patel BK, Eckstein F (1998) Incorporation of terminal phosphorothioates into oligonucleotides. *Nucleic Acids Res* 26:4983–4988.
10. Vagin VV, et al. (2006) A distinct small RNA pathway silences selfish genetic elements in the germline. *Science* 313:320–324.
11. Cerutti H, Johnson AM, Gillham NW, Boynton JE (1997) Epigenetic silencing of a foreign gene in nuclear transformants of Chlamydomonas. *Plant Cell* 9:925–945.

12. Zhang C, Wu-Scharf D, Jeong B-R, Cerutti H (2002) A WD40-repeat containing protein, similar to a fungal co-repressor, is required for transcriptional gene silencing in Chlamydomonas. *Plant J* 31:25–36.
13. Varagona MJ, Schmidt RJ, Raikhel NV (1992) Nuclear localization signal(s) required for nuclear targeting of the maize regulatory protein Opaque-2. *Plant Cell* 4:1213–1227.
14. Ibrahim F, Rohr J, Jeong WJ, Hesson J, Cerutti H (2006) Untemplated oligoadenylation promotes degradation of RISC-cleaved transcripts. *Science* 314:1893.
15. Lange H, et al. (2008) Degradation of a polyadenylated rRNA maturation by-product involves one of the three RRP6-like proteins in Arabidopsis thaliana. *Mol Cell Biol* 28: 3038–3044.

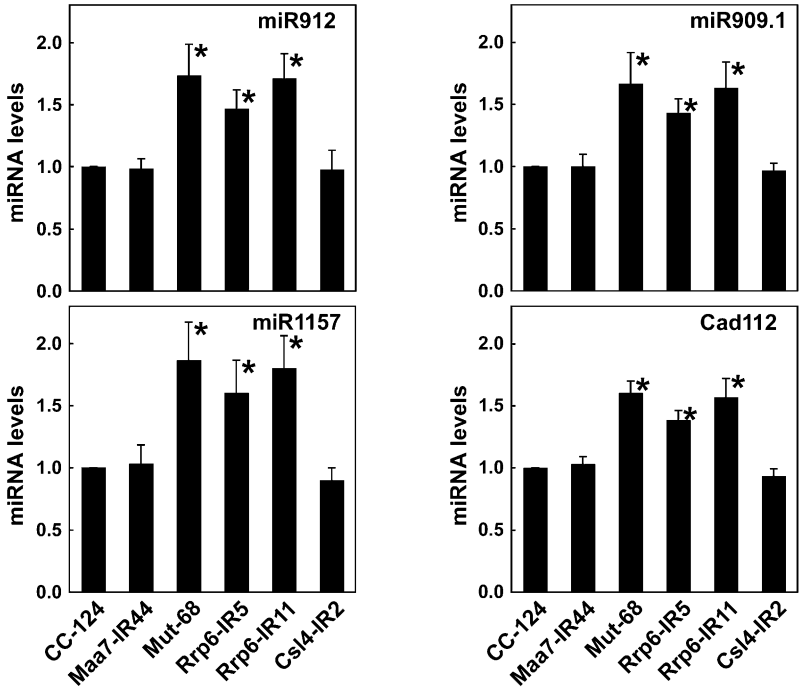

Fig. S1. Mut-68, a mutant defective in the nucleotidyltransferase MUT68, and strains depleted for the RRP6 exosome subunit show increased levels of miRNAs. The histograms display the relative abundance of small RNAs detected by Northern blotting with probes specific for the indicated *Chlamydomonas* miRNAs and normalized to the amount of the U6 small nuclear RNA. Cad112, candidate miRNA 112 (7). For illustration purposes, the miRNA levels in the wild-type strain (CC-124) were set to 1.0 and the remaining samples were then adjusted accordingly. The results shown are the average of four independent experiments ± the standard deviation. Samples marked with an asterisk are significantly different ($P < 0.05$) from the parental transgenic strain (Maa7-IR44) in a two-tailed Student's *t* test. CC-124, wild-type strain; Maa7-IR44, CC-124 transformed with an IR transgene designed to induce RNAi of *MAA7* (encoding tryptophan synthase β subunit); Mut-68, *MUT68* deletion mutant; Rrp6-IR5 and Rrp6-IR11, Maa7-IR44 transformed with IR transgenes inducing RNAi of two distinct genes encoding the RRP6 exosome subunit; Csl4-IR2, strain transformed with an IR transgene triggering RNAi of *CSL4* (encoding a core exosome subunit).

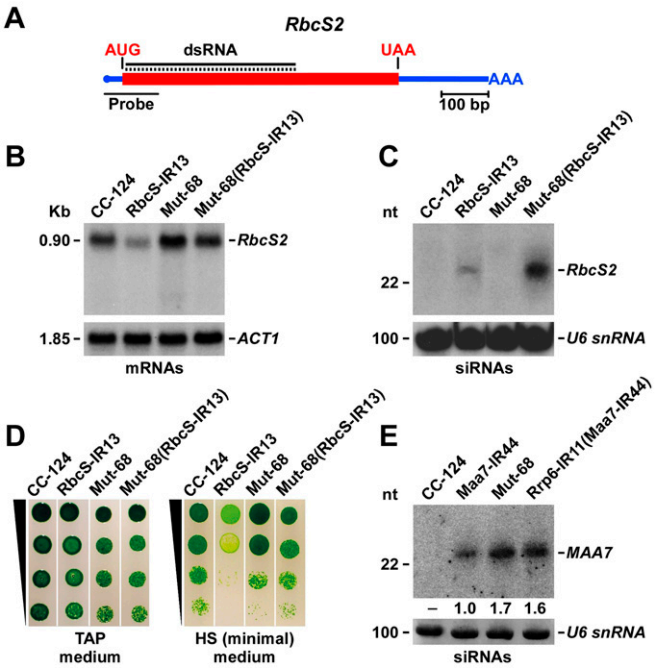

Fig. S2. Mut-68 and strains depleted for the RRP6 exosome subunit show enhanced levels of small interfering RNAs (siRNAs). (*A*) Schematic representation of the *RbcS2* transcript (encoding RUBISCO, an essential enzyme for photosynthetic CO_2 fixation). The regions of homology to a dsRNA from an inverted repeat (IR) transgene, triggering RNAi, and to the probe used for Northern blot hybridization are indicated by black lines. (*B*) Northern blot analysis of total RNA isolated from the indicated strains. The same filter was sequentially hybridized with probes specific for the 5′ end of the *RbcS2* transcript and the *ACTIN1* 3′-UTR sequence. CC-124, wild-type strain; RbcS-IR13, CC-124 transformed with an IR transgene designed to induce RNAi of *RbcS2* (1); Mut-68, *MUT68* deletion mutant (14); Mut-68(RbcS-IR13), Mut-68 containing the *RbcS2* IR transgene introduced by crossing. (*C*) Detection of *RbcS2* siRNAs by Northern blotting. A representative blot out of three replicates is shown. Hybridization to the U6 small nuclear RNA was used as a control for equivalent loading of the lanes. (*D*) Growth and survival of the indicated strains on Tris-acetate-phosphate (TAP) medium or on high salt (HS) minimal medium. Cells with RNAi-mediated suppression of RUBISCO are deficient in photosynthesis and grow very poorly on HS medium. (*E*) Northern blot analysis of siRNAs corresponding to the *MAA7* gene (encoding tryptophan synthase β subunit). Maa7-IR44, CC-124 transformed with an IR transgene designed to induce RNAi of *MAA7*; Mut-68 was isolated in the Maa7-IR44 background and already contains the *MAA7* IR transgene (14); Rrp6-IR11(Maa7-IR44), Maa7-IR44 transformed with an IR transgene inducing RNAi-mediated depletion of the RRP6 exosome subunit. The numbers below the blot indicate the relative abundance of the siRNAs. A representative blot out of three replicates is shown.

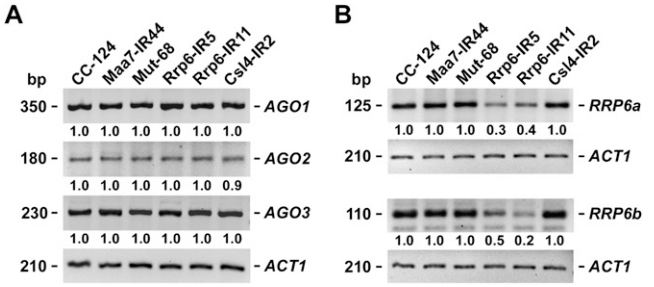

Fig. S3. Analysis of the steady-state mRNA levels corresponding to the *ARGONAUTE* and *RRP6* genes by reverse transcriptase (RT)-PCR. (*A*) RT-PCR analysis of *AGO1*, *AGO2*, and *AGO3* expression in the indicated strains. Amplification of *ACT1* (encoding actin) transcripts is shown as an input control. The numbers below the panels indicate the relative abundance of the PCR products. Representative gels out of four replicates are shown. Reactions using RNA not treated with reverse transcriptase as the template were employed as a negative control (data not shown). CC-124, wild-type strain; Maa7-IR44, CC-124 transformed with an IR transgene designed to induce RNAi of *MAA7* (encoding tryptophan synthase β subunit); Mut-68, *MUT68* deletion mutant (14); Rrp6-IR5 and Rrp6-IR11, Maa7-IR44 transformed with IR transgenes inducing RNAi of two distinct genes encoding the RRP6 exosome subunit; Csl4-IR2, strain transformed with an IR transgene triggering RNAi of *CSL4* (encoding a core exosome subunit). (*B*) RT-PCR analysis of *RRP6a* and *RRP6b* expression in the indicated strains. The numbers below the panels indicate the relative abundance of the PCR products. Representative gels out of four replicates are shown. The *Chlamydomonas* genome contains two genes coding for homologs of the RRP6 exosome subunit (including both 3′-to-5′ exonuclease and HRDC domains): *RRP6a* (511862; au5.g2165_t1) and *RRP6b* (284930; au.g3315_t1) (http://genome.jgi-psf.org/Chlre4/Chlre4.home.html). The transgene introduced into Rrp6-IR5 was designed to suppress specifically *RRP6a* whereas the transgene introduced into Rrp6-IR11 was designed to knock down *RRP6b*. However, because of the sequence identity between these two *RRP6* paralogs, each IR construct suppresses, to different degrees, the expression of both *RRP6* genes.

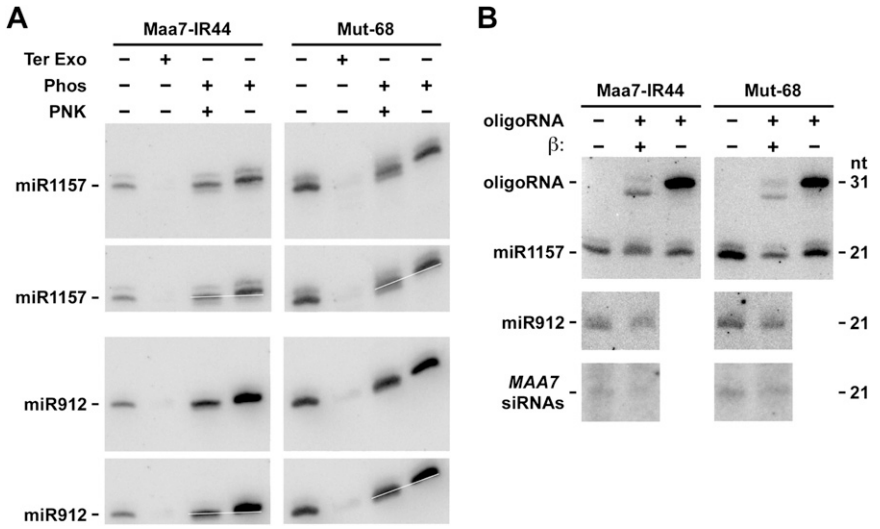

Fig. S4. Northern analysis of enzymatic and chemical probing of small RNA ends. (*A*) 5′ end analysis of small RNAs. Purified sRNAs were treated with terminator exonuclease (Ter Exo), alkaline phosphatase (Phos), or alkaline phosphatase followed by T4 polynucleotide kinase (PNK). After separation by denaturing PAGE, miR1157 was detected by Northern hybridization. The membrane was then stripped and reprobed for miR912. The susceptibility of the miRNAs to degradation by Terminator Exonuclease and the slight mobility shift caused by alkaline phosphatase (which was reversed by PNK) are consistent with miR1157 and miR912 having a 5′ monophosphate terminus. (*B*) 3′ end analysis of small RNAs. Purified sRNA samples, mixed with 0.05 pmol of an unmodified 31-mer oligoRNA partly homologous to miR1157, were subjected to periodate oxidation and β-elimination reactions. After separation by denaturing PAGE, small RNAs were electroblotted to a nylon membrane and detected by sequential hybridization with probes specific for miR1157, miR912, and *MAA7* siRNAs. Representative blots out of three replicates are shown. Whereas most of the synthetic oligoRNA migrates faster following β-elimination, the miRNAs and siRNAs do not appear to be affected, indicating lack of a 2′,3′ hydroxy terminus. These results are consistent with methylation at the 2′ hydroxy position of the 3′ terminal nucleotide in *Chlamydomonas* small RNAs and with the existence of a functional HEN1 homolog, as previously reported (6).

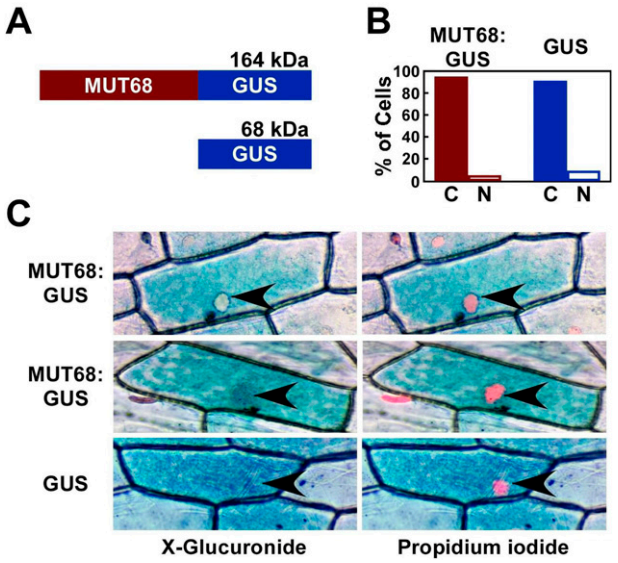

Fig. S5. Subcellular localization of GUS and MUT68-GUS fusion proteins in transiently transformed onion epidermal cells. (*A*) Diagram of GUS and of the MUT68-GUS fusion polypeptides. (*B*) The proteins expressed in onion epidermal cells were localized histochemically by the X-glucuronide assay. Transformed cells were classified as showing nuclear localization of GUS activity (empty bars, N) or not (solid bars, C). The results shown are the average of three independent experiments (n = 300 for each construct). (*C*) Representative cellular staining patterns in transiently transformed onion cells. Tissues were simultaneously analyzed by X-glucuronide staining (blue color, *Left*) and nuclei-specific propidium iodide staining (orange color, *Right*). The *Upper* and *Middle* panels correspond to cells transformed with the MUT68-GUS fusion protein whereas the bottom panel corresponds to a cell transformed with GUS alone. The *Middle* panel is shown as an example of the nuclear localization of MUT68-GUS although the frequency of these events was very low. The nuclei are indicated with arrowheads. The subcellular localization of the *Chlamydomonas* RRP6 exosome subunits was not determined but in *Arabidopsis thaliana*, which contains three RRP6-like proteins, one isoform is restricted to the cytoplasm and the other two show distinct intranuclear localizations (15).

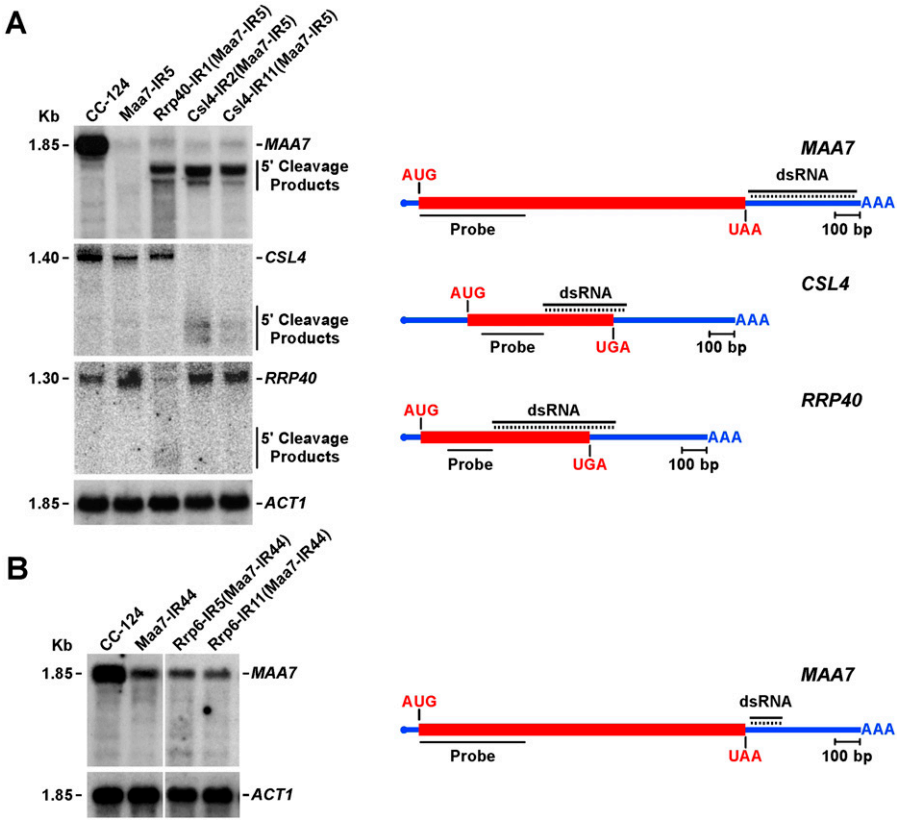

Fig. S6. RNAi-mediated depletion of the CSL4 or RRP40, but not of the RRP6, exosome subunits partly stabilizes the 5′ RNA fragments resulting from siRNA-directed cleavage. (*A*) Northern blot analysis of the MAA7, CSL4, or RRP40 transcripts in the indicated strains. Schematic representations of the cognate mRNAs are shown on the Right. The regions of homology to the dsRNA triggers and to the probes used for northern blot hybridization are indicated by black lines. CC-124, wild type strain; Maa7-IR5, transgenic strain with RNAi-suppressed MAA7 (1); Rrp40-IR1(Maa7-IR5), double transgenic strain generated by transforming Maa7-IR5 with an IR construct homologous to the RRP40 mRNA; Csl4-IR2(Maa7-IR5) and Csl4-IR11(Maa7-IR5), double transgenic strains generated by transforming Maa7-IR5 with an IR construct homologous to the CSL4 mRNA. Hybridization to the ACTIN1 mRNA was used as a control for equivalent loading of the lanes. (*B*) Northern blot analysis of the MAA7 transcript in strains suppressed for the RRP6 exosome subunit. The panels correspond to non-consecutive lanes from the same blot. Note the lack of stabilization of the 5′ RNA products generated by siRNA-directed cleavage.

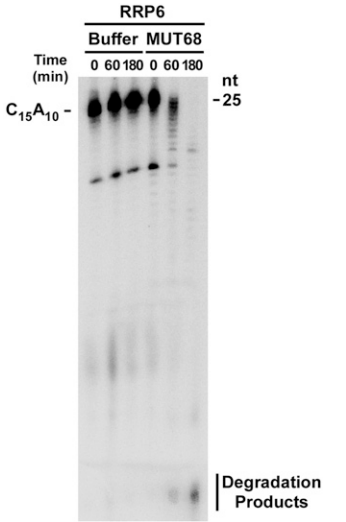

Fig. S7. Recombinant MUT68 promotes the in vitro degradation of oligoribonucleotides by the RRP6 exosome subunit. A $C_{15}A_{10}$ oligoRNA, ^{32}P-labeled at its 5′ end, was incubated with affinity-purified RRP6 alone (buffer) or with the addition of MUT68. Reactions were stopped at the indicated times, separated by denaturing PAGE, and analyzed by autoradiography. The gel was run for a short time to examine the accumulation of degradation products, which were run off the gels shown in Fig. 2 *C*–*E*. Incubation with MUT68 alone for up to 180 min did not result in the accumulation of degradation products, indicating that recombinant MUT68 did not contain contaminating ribonuclease activity (data not shown).

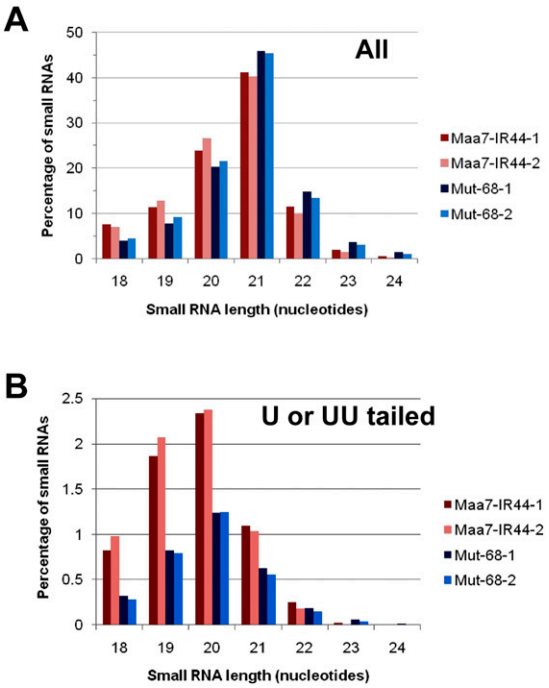

Fig. S8. Analysis of endogenous small RNA sizes in Mut-68 and the parental strain Maa7-IR44. (*A*) Size distribution of unique (distinct) small RNAs, after subtracting putative degradation products and normalization. Two independent libraries were examined for each strain. Unique sRNA sequences from Maa7-IR44 are represented by red (Maa7-IR44-1) or pink (Maa7-IR44-2) bars. Unique sRNA sequences from Mut-68 are represented by blue (Mut-68-1) or light blue (Mut-68-2) bars. The number following the strain names indicates the small cDNA library from which the data were obtained. (*B*) Size distribution of unique small RNAs with an untemplated 3′ terminal U or UU (after removing the tails). Two independent libraries were examined for each strain and the bars are colored as indicated above (*A*).

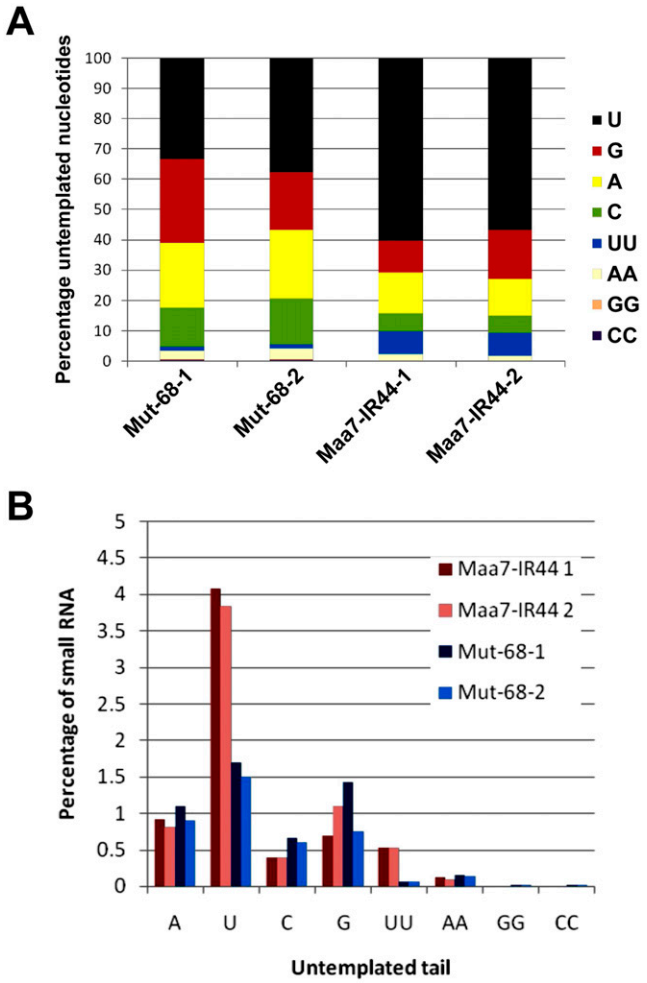

Fig. S9. Analysis of untemplated nucleotide additions to the 3′ termini of small RNAs in Mut-68 and the parental strain Maa7-IR44. (*A*) Frequency of the predominant untemplated nucleotides added to the 3′ ends of small RNAs (relative to all sRNAs with 3′ nucleotide additions). Two independent libraries were examined for each strain and the number following the strain names indicates the small cDNA library from which the data were obtained. (*B*) Frequency of small RNAs (as a percentage of all sRNAs) with 3′ untemplated nucleotide additions in Mut-68 and the parental strain Maa7-IR44.

Other Supporting Information Files

Dataset S1 (XLS)